University of Pennsylvania
ScholarlyCommons

Department of Physics Papers | Department of Physics

10-6-2008

# Energy of *K*-Momentum Dark Excitons in Carbon Nanotubes by Optical Spectroscopy

Omar N. Torrens
*University of Pennsylvania*

Ming Zheng
*DuPont Central Research and Development*

James M. Kikkawa
*University of Pennsylvania*, kikkawa@physics.upenn.edu

Suggested Citation:
O.N. Torrens, M. Zheng, and J.M. Kikkawa. (2008). "Energy of K-Momentum Dark Excitons in Carbon Nanotubes by Optical Spectroscopy." *Physical Review Letters.* **101**, 157401.

© 2008 The American Physical Society
http://dx.doi.org/10.1103/PhysRevLett.101.157401

This paper is posted at ScholarlyCommons. http://repository.upenn.edu/physics_papers/90
For more information, please contact repository@pobox.upenn.edu.

# Energy of *K*-Momentum Dark Excitons in Carbon Nanotubes by Optical Spectroscopy

**Abstract**
Phonon sideband optical spectroscopy determines the energy of the dark *K*-momentum exciton for (6,5) carbon nanotubes. One-phonon sidebands appear in absorption and emission, split by two zone-boundary (*K*-point) phonons. Their average energy locates the $E_{11}$ *K*-momentum exciton 36 meV above the $E_{11}$ bright level, higher than available theoretical estimates. A model for exciton-phonon coupling shows the absorbance sideband depends sensitively on the *K*-momentum exciton effective mass and has minimal contributions from zone-center phonons, which dominate the Raman spectra of carbon nanotubes.

**Disciplines**
Physical Sciences and Mathematics | Physics

**Comments**
Suggested Citation:
O.N. Torrens, M. Zheng, and J.M. Kikkawa. (2008). "Energy of K-Momentum Dark Excitons in Carbon Nanotubes by Optical Spectroscopy." *Physical Review Letters.* **101**, 157401.

© 2008 The American Physical Society
http://dx.doi.org/10.1103/PhysRevLett.101.157401

This journal article is available at ScholarlyCommons: http://repository.upenn.edu/physics_papers/90

# Energy of $K$-Momentum Dark Excitons in Carbon Nanotubes by Optical Spectroscopy

O. N. Torrens,[1] M. Zheng,[2] and J. M. Kikkawa[1,*]

[1]Department of Physics and Astronomy, University of Pennsylvania, Philadelphia, Pennsylvania 19104, USA
[2]DuPont Central Research and Development, Experimental Station, Wilmington, Delaware 19880, USA

(Received 11 September 2007; published 6 October 2008)

Phonon sideband optical spectroscopy determines the energy of the dark $K$-momentum exciton for (6,5) carbon nanotubes. One-phonon sidebands appear in absorption and emission, split by two zone-boundary ($K$-point) phonons. Their average energy locates the $E_{11}$ $K$-momentum exciton 36 meV above the $E_{11}$ bright level, higher than available theoretical estimates. A model for exciton-phonon coupling shows the absorbance sideband depends sensitively on the $K$-momentum exciton effective mass and has minimal contributions from zone-center phonons, which dominate the Raman spectra of carbon nanotubes.

DOI: 10.1103/PhysRevLett.101.157401 PACS numbers: 78.30.Na, 73.22.Lp, 78.67.Ch

Unlike the "particle in a box," excitons in semiconducting carbon nanotubes (CNTs) have energies that do not vary monotonically with the confinement length (i.e., tube diameter). Instead, elaborate patterns emerge when the energies of optically active excitons are compared for different nanotube species, identified by their wrapping vector ($n$, $m$) [1,2]. These patterns of "bright" exciton energies are historically important scientific developments, providing a connection between optical transitions and atomic structure [1] and underscoring the importance of electron-electron interactions within this context [3]. The manifold of optically inactive "dark" states actually contains more information than the bright manifold, but is more difficult to study since it does not couple directly to light [4,5]. Methods that allow one to map dark exciton energies across the entire CNT family will almost certainly bring a deeper understanding of CNT electronic structure, and may also inform a host of unexplained phenomena in CNT photophysics including unidentified transitions [6], intertube energy transfer [7], and variations of optical properties between samples, molecules, and different sections of the same molecule [8].

Thus far, researchers have combined high magnetic field photoluminescence (PL) with an assumption that the exciton manifold is thermalized to infer the energy of the zero-momentum dark singlet exciton [4,5]. Yet there are two remaining dark singlets whose energies remain experimentally undetermined. These states have center-of-mass momenta near the graphite $K$ and $K'$ points (Fig. 1, inset), are degenerate by time-reversal symmetry [9], and are heretofore collectively referred to as $K$-momentum singlet excitons. Because of their large momenta, $K$-momentum singlets cannot couple directly to photons. However, through a second order process involving exciton-phonon coupling [10], photons can create or destroy $K$-momentum singlets *and* phonons.

In this Letter, we exploit this coupling to determine the energy of the $K$-momentum singlets. Using PL, absorbance, and Raman spectroscopies on room-temperature CNT suspensions, we study two optical sidebands of the main transition of the (6,5) species. Our observations, made possible by high single-species enrichment [11] and by the statistics of an ensemble measurement, show the sidebands to be asymmetrically positioned about the zero-phonon peaks and thus are not zero-momentum ($\Gamma$-point) phonon sidebands of the bright exciton. Instead, the sidebands are identified as *bright* sidebands of the *dark* $K$-momentum exciton, which result from mixing among singlets via exciton-phonon coupling. The av-

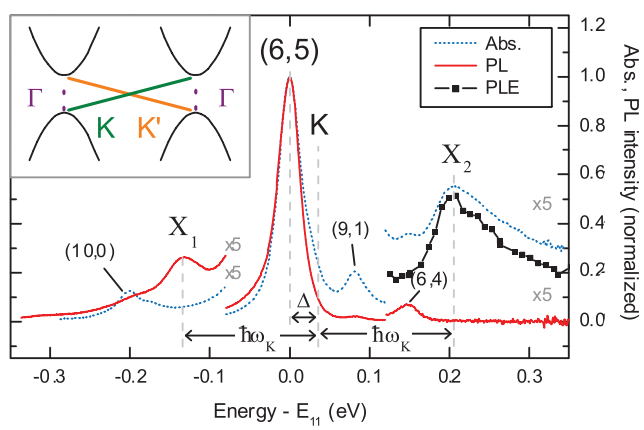


FIG. 1 (color). Resonant PL (solid red line), absorbance (dotted blue line), and PLE (dot-dashed line) showing bright phonon sidebands $X_1$ and $X_2$ of the (6,5) $E_{11}$ dark $K$-momentum singlet. Minority ($n$, $m$) CNT species are assigned as labeled [31]. Label $K$ is the inferred energy of the degenerate $K$- and $K'$-momentum excitons, $\Delta$ is their splitting from $E_{11}$, and $\hbar\omega_K$ represents the $K$-point phonon energy separating $X_1$ and $X_2$ from $K$. (inset) A schematic of the direct and indirect electron-hole pairs that comprise $\Gamma$- and $K$-momentum excitons, respectively. For PL excitation was $2.190 \pm 0.046$ eV ($E_{22}$). For PLE, excitation scanning near $E_{11}$ uses a tungsten halogen lamp to avoid arc-lamp spikes near $X_2$. Detector FWHM for absorbance, PL, and PLE is 3, 6, and 6 meV, respectively. The abscissas are centered on the $E_{11}$ peaks, 1.258 eV for absorbance and PLE, and 1.253 eV for PL.

 © 2008 The American Physical Society

erage energy of these sidebands locates the $K$-momentum singlets at $\Delta = 36$ meV *above* the lowest-energy bright state for the (6,5) CNT, in contrast to recent work in which the upper energy (absorbance) sideband was assumed to be a $\Gamma$-point phonon sideband, and the lower energy (PL) sideband was interpreted as a "deep excitonic" state located energetically *below* the bright exciton (and therefore perhaps responsible for low CNT quantum yields) [12]. This splitting $\Delta$ is, to our knowledge, the first such spacing experimentally determined for any $(n, m)$ species and shows that theoretical predictions have somewhat underestimated $\Delta$. Our technique is applicable to any semiconducting CNT species and provides a strategy toward fully mapping the $(n, m)$-dependency of $\Delta$.

Our sample is an aqueous dispersion of DNA-wrapped [13] CoMoCAT CNTs [14] sorted by ion-exchange chromatography [15] to enrich the ensemble in primarily the (6,5) species. Additionally, we have added sodium deoxycholate (1 wt%) to reduce inhomogeneous broadening [16]. Magnetic alignment and PL measurements on similarly prepared samples show excellent single-tube dispersion [7]. The pink-colored sample has a peak optical density of 1.1 $\mathrm{cm}^{-1}$ at the (6,5) absorption resonance. Except where noted, PL is excited by the output of an arc lamp and monochromator, collected perpendicular to the excitation, and guided into a spectrometer with a thermoelectrically cooled InGaAs array. All PL are corrected for spectral detection sensitivity and excitation powers ($\leq 65$ $\mu$W). Absorbance spectra are taken with the same spectrometer using a tungsten lamp. Raman scattering uses the frequency doubled, line-filtered output of a Nd:YAG laser.

A combination of PL and absorbance spectroscopy is often used in molecular and solid-impurity studies to identify phonon-assisted optical transitions [17]. At temperatures much lower than the phonon energies, such peaks appear only at higher energy in absorbance and only at lower energy in PL, with respect to the zero-phonon transition. Identifying complementary pairs of such transitions in CNTs has been difficult in typical samples, which can have impurities and multiple $(n, m)$ species with strong, overlapping optical transitions.

PL and absorbance spectra in our (6,5)-enriched sample reveal two weak but observable peaks (denoted $X_1$ and $X_2$) that we ultimately assign as complementary phonon sidebands of the (6,5) $E_{11}$ $K$-momentum exciton. The central peak in both curves (Fig. 1) corresponds to the (6,5) bright $E_{11}$ exciton, and the other resonances are well accounted for by other chiralities [1] except $X_1$ and $X_2$. Appearing at 0.206 eV above the bright singlet (but missing from PL), $X_2$ is consistent with an absorbance phonon sideband. Moreover, $X_2$ is not due to impurities, having been directly observed in a single-molecule study [18], while an equivalent sideband was shown to have a lattice origin in a $^{13}$C isotope study [19]. Photoluminescence excitation spectra (PLE) show an excitation peak at $X_2$ when detection is tuned to the (6,5) $E_{11}$ bright exciton transition (Fig. 1), confirming that $X_2$ is associated with absorption into the (6,5) species. In PL, $X_1$ is also consistent with a phonon sideband, since this feature (at 0.134 eV below the bright singlet) does not appear in absorbance and is intrinsic to the (6,5) CNT: Fig. 2, which plots the excitation energy dependence of the PL spectra, shows that $X_1$ has the same excitation resonance as the (6,5) species.

What distinguishes $X_1$ and $X_2$ from typical phonon sidebands are their asymmetric positions relative to the (6,5) $E_{11}$ bright exciton (Fig. 1). To first approximation, sidebands are symmetric [20], with an absorbance sideband energy $E_{X_2}$ equal to $E_{\mathrm{exciton}} + \hbar\omega_{\mathrm{phonon}}$, and a PL sideband energy $E_{X_1} = E_{\mathrm{exciton}} - \hbar\omega_{\mathrm{phonon}}$. Peaks $X_1$ and $X_2$ are therefore most naturally assigned to bright phonon sidebands of a dark (i.e., unobserved) exciton state. This dark state has an energy $(E_{X_1} + E_{X_2})/2$, and is therefore at $\Delta = 36$ meV above the bright level (Fig. 1).

The particular exciton state that $\Delta$ locates is the $K$-momentum singlet (Fig. 1), an assignment supported by the energetic splitting between $X_1$ and $X_2$. Figure 3 shows the Stokes Raman spectrum of our sample with the two strongest peaks $G$ and $2D$ at $-0.197$ and $-0.326$ eV, respectively. In CNTs, these peaks derive from graphitelike vibrations, with the former mainly from $\Gamma$-point longitudinal optical (LO) modes [21] and the latter from two-phonon scattering involving totally symmetric ($A_1'$) modes at the $K$ point [22]. The $X_2 - X_1$ splitting (Fig. 1) is too small to be accounted for by two $\Gamma_{\mathrm{LO}}$ phonons, but matches well the two-phonon energy of the $2D$ peak (Fig. 3). Thus, the individual energies of the $X_1$ and $X_2$ peaks (Fig. 1) are each consistent with those of single $K_{A_1'}$ phonons. Combining PL with absorbance allows us to identify both the central energy and splitting of these phonon sidebands, which is impossible when only one sideband is observed [18,19,23,24].

Our theoretical calculations bolster these conclusions, predicting that $K_{A_1'}$ modes not only have the largest cou-

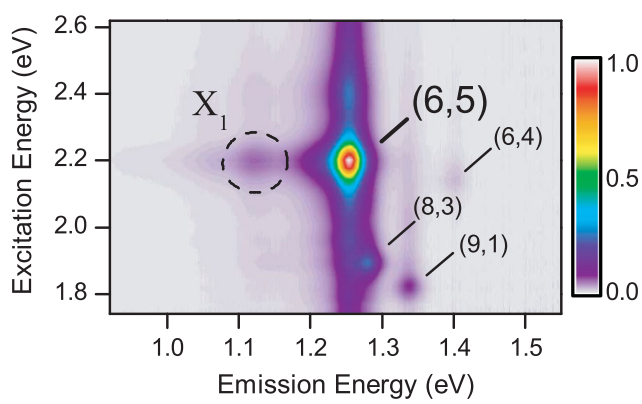


FIG. 2 (color). Normalized PL intensity vs excitation and emission energies. $X_1$ is the bright phonon sideband of the dark (6,5) $E_{11}$ $K$-momentum exciton. Excitation bandwidth and detection resolution are 38 meV FWHM and 13 meV FWHM, respectively, at the main (6,5) resonance.

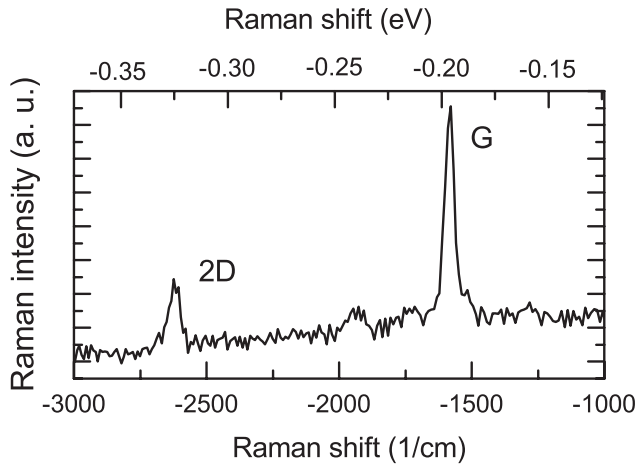


FIG. 3. Stokes Raman scattering spectrum taken at 2.330 eV excitation. $2D$ arises from two $K$-point $A_1'$-symmetry phonons and $G$ arises predominantly from one $\Gamma$-point LO phonon.

pling of any modes in (6,5) CNTs, but also that the $K$-momentum exciton effective mass results in a uniquely strong $K$-momentum phonon sideband peak intensity. CNT exciton-phonon couplings, which mix excitons of different center-of-mass momenta, can be expressed as $B_{q\mu}^{SS'} = \sum_k M_{k,q}^{\mu} A_{k,q}^{S'*}(A_{k,0}^{S} + A_{k+q,0}^{S})$, where $A_{q,k}^{S}$ are the exciton wave function coefficients for electron-hole relative momentum $q$, center-of-mass momentum $k$, and $S = 0, 1, \ldots$ labels the ground, first excited, etc. states of the exciton, while $M_{k,q}^{\mu}$ is the electron-phonon coupling for phonon band $\mu = 1, 2, \ldots, 6$ [10]. In order to find $B_{q\mu}^{SS'}$ for (6,5) CNTs, we calculate the $A_{k,q}^{S}$ coefficients by the method of Jiang *et al.*, which uses a tight-binding basis (2.7 eV nearest-neighbor coupling) and solves the Bethe-Salpeter equation [25]. The environmental dielectric constant is set to $\epsilon = 2.7$ in order to bring the calculated (6,5) $E_{11}$ bright exciton energy into agreement with our measured value of $\sim$1.25 eV (Fig. 2). We calculate the electron-phonon couplings $M_{k,q}^{\mu}$ to first order in the lattice deformations [26], with a nearest-neighbor tight-binding coupling constant of 5.3 eV/Å. We determine the phonon eigenmodes and eigenfrequencies within a symmetry-adapted force-constant model [27] using graphite force-constants up to 5th nearest neighbors [28].

The $E_{11}$ bright exciton absorbance $I(\omega)$ includes the unperturbed, "zero-phonon" peak, as well as contributions due to exciton-phonon mixing. A perturbative expansion yields the expression

$$I(\omega) \propto \delta(E_{11} - \hbar\omega) + \sum_{q,\mu,S'} \frac{|B_{q\mu}^{0S'}|^2}{(E_q^{S'} + \hbar\omega_{-q}^{\mu} - E_{11})^2} \times \delta(E_q^{S'} + \hbar\omega_{-q}^{\mu} - \hbar\omega), \quad (1)$$

where $E_q^{S'}$ are the exciton energies, $\omega_{-q}^{\mu}$ are the phonon eigenfrequencies, and $E_{11}$ is the bright exciton energy [10]. Figure 4(a) compares the amplitude of the resulting (6,5) sideband spectrum with the absorbance data of Fig. 1. In addition to the full sum [Eq. (1)], which ranges over six modes near $\Gamma$ and six near $K$, we plot the contribution of just the $K_{A_1'}$ mode. The spectra show first that the theoretical (6,5) $I(\omega)$ agrees reasonably well with the measured intensity of peak $X_2$, and second that the $K_{A_1'}$ mode accounts for nearly the entire sideband. Hence, we can conclude that for the (6,5) CNT, theory supports our assignment of the $X_1$ and $X_2$ peaks [Fig. 4(a)] as phonon sidebands centered about the $K$-momentum singlet.

Notably, both the theory of Fig. 4(a) and the data of Fig. 1 imply that although $\Gamma$-point phonons figure prominently in CNT Raman scattering (Fig. 3), they do not produce a significant sideband of the (6,5) $E_{11}$ bright exciton [10]. The relevant $\Gamma_{\rm LO}$ mode is included in $I(\omega)$ with a calculated exciton-phonon coupling $B_{q\mu}^{0S'}$ approximately half that of the $K_{A_1'}$ mode. Nevertheless, its relative contribution is insignificant. To understand this behavior, we note that the term $\delta(E_q^{S'} + \hbar\omega_{-q}^{\mu} - \hbar\omega)$ in Eq. (1) makes the sideband peak intensity depend sensitively on the composite density of states (DOS) of the $E_q^{S'} + \hbar\omega_{-q}^{\mu}$ band. Optical phonon dispersions $\hbar\omega_{-q}^{\mu}$ are nearly flat near $K$ and $\Gamma$, so the composite DOS is chiefly determined by the $K$-momentum and bright $E_{11}$ dispersions, respectively. Bright excitons have relatively small effective masses, so $\Gamma_{\rm LO}$ phonons contribute little to the phonon sideband peak intensity.

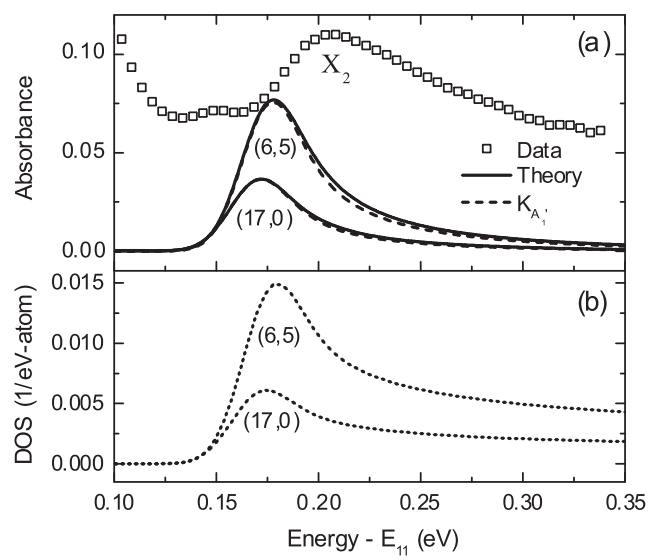


FIG. 4. (a) Amplitude comparison of phonon sideband absorbance data (squares) and model predictions $I(\omega)$ (solid lines). The latter are calculated for the (6,5) and (17,0) CNTs. For both CNTs, the $K_{A_1'}$ (dashed lines) contributions are also plotted. Energetic discrepancies between data and fit are explained in the text and do not affect our determination of $\Delta$. (b) Density of states of the sum of the lowest-energy $E_{11}$ $K$-momentum exciton and $K_{A_1'}$ phonon bands for the (6,5) and (17,0) CNTs. All theoretical curves in (a) and (b) are 30 meV Gaussian broadened.

Many of the aforementioned conclusions also apply to the (17,0) CNT, which is shown for comparison in Fig. 4 and is discussed in Ref. [10]. Interestingly, although our calculated exciton-phonon couplings for the (6,5) and (17,0) species are nearly identical, their sideband peak intensities are appreciably different [Fig. 4(a)]. These differences are again explained by composite DOS considerations. Figure 4(b) plots the $K$-momentum exciton-phonon DOS for the (6,5) and (17,0) species. Here DOS $= \sum_q \delta(E_q + \hbar\omega_{-q} - \hbar\omega)$, the phonon energies $\hbar\omega_{-q}$ are from the $K_{A_1'}$ dispersion, and the exciton energies $E_q$ are from the lowest-energy $K$-momentum exciton dispersion. The DOS differences in Fig. 4(b) largely account for the predicted sideband intensity differences of Fig. 4(a), suggesting that the $K$-momentum exciton effective mass (rather than exciton-phonon coupling) determines variations in $K_{A_1'}$ sideband peak intensity between different $(n, m)$ CNTs.

A recent theoretical study found $\Delta$ to vary strongly with $(n, m)$ index, ranging from 8 to 48 meV for semiconducting CNTs within the 0.6 to 1 nm diameter range and an environmental dielectric constant of $\epsilon = 1.846$ [29]. For the (6,5) CNT, the prediction is $\Delta = 23$ meV, which we can bring into agreement with our measured value of 36 meV, but only by setting $\epsilon = 1.33$ (thus rescaling the bright and $K$-momentum binding energies [30]). Values for $\epsilon$ that best match experimental observations range from 2.2 [25] to 3.2 [29], so $\epsilon = 1.33$ is likely inconsistent with the aqueous environment of our CNTs. Hence, the prediction [29] appears to underestimate $\Delta$ for the (6,5) species. We note that in the course of solving the Bethe-Salpeter equation for the exciton dispersions $E_q^{S'}$ used in Eq. (1), the model we employed (the simple tight-binding model in Ref. [25]) produced $\Delta = 10$ meV (also an underestimate), which is the primary reason for the mismatch in peak energies between the absorbance data and theory (Fig. 4). Given that the relative splittings among excitons depend on the parametrization of the Coulomb interaction (e.g., $w_1$ and $w_2$ in Ref. [9]), our results may guide theoretical approximations for CNTs in general.

In conclusion, we have observed a pair of phonon sidebands in absorbance and PL that, in our (6,5)-enriched ensemble, locates the $K$-momentum singlet at $\Delta =$ 36 meV above the $E_{11}$ bright exciton. Raman data support the peak assignments as bright $K$-momentum phonon sidebands of the dark $K$-momentum exciton, and a nearest-neighbor tight-binding calculation points to the importance of the exciton effective mass in explaining both the absence of observed $\Gamma$-point phonon sidebands and the sideband intensity differences between CNT species with similar exciton-phonon coupling strengths. In particular, we find that the $X_2$ sideband displacement approximates the energy of $\Gamma$-point phonons is apparently coincidental. Further studies may include systematically probing correlations among $\Delta$, phonon sideband intensity, and PL efficiency in the (6,5) and other $(n, m)$ species.

We thank E. J. Mele for useful discussions and NSF MRSEC Grant No. DMR-0520020 for support.

*kikkawa@physics.upenn.edu

[1] S. M. Bachilo *et al.*, Science **298**, 2361 (2002).
[2] P. T. Araujo *et al.*, Phys. Rev. Lett. **98**, 067401 (2007).
[3] C. L. Kane and E. J. Mele, Phys. Rev. Lett. **90**, 207401 (2003).
[4] I. B. Mortimer and R. J. Nicholas, Phys. Rev. Lett. **98**, 027404 (2007).
[5] J. Shaver *et al.*, Nano Lett. **7**, 1851 (2007).
[6] J. Lefebvre, P. Finnie, and Y. Homma, Phys. Rev. B **70**, 045419 (2004).
[7] O. N. Torrens *et al.*, Nano Lett. **6**, 2864 (2006).
[8] J. Lefebvre *et al.*, Nano Lett. **6**, 1603 (2006).
[9] T. Ando, J. Phys. Soc. Jpn. **75**, 024707 (2006).
[10] V. Perebeinos, J. Tersoff, and P. Avouris, Phys. Rev. Lett. **94**, 027402 (2005).
[11] M. Zheng and E. D. Semke, J. Am. Chem. Soc. **129**, 6084 (2007).
[12] O. Kiowski *et al.*, Phys. Rev. Lett. **99**, 237402 (2007); S. Lebedkin *et al.*, Phys. Rev. B **77**, 165429 (2008).
[13] M. Zheng *et al.*, Nature Mater. **2**, 338 (2003).
[14] B. Kitiyanan *et al.*, Chem. Phys. Lett. **317**, 497 (2000).
[15] M. Zheng *et al.*, Science **302**, 1545 (2003).
[16] E. S. Jeng *et al.*, Nano Lett. **6**, 371 (2006).
[17] See, for example J. B. Birks and D. J. Dyson, Proc. R. Soc. A **275**, 135 (1963).
[18] S. Berciaud *et al.*, Nano Lett. **7**, 1203 (2007).
[19] Y. Miyauchi and S. Maruyama, Phys. Rev. B **74**, 035415 (2006).
[20] C. S. Kelley, Phys. Rev. B **8**, 1806 (1973).
[21] M. Dresselhaus *et al.*, Phys. Rep. **409**, 47 (2005).
[22] F. Tuinstra and J. L. Koenig, J. Chem. Phys. **53**, 1126 (1970).
[23] F. Plentz *et al.*, Phys. Rev. Lett. **95**, 247401 (2005).
[24] J. U. Lee, P. J. Codella, and M. Pietrzykowski, Appl. Phys. Lett. **90**, 053103 (2007).
[25] J. Jiang *et al.*, Phys. Rev. B **75**, 035407 (2007).
[26] L. Pietronero *et al.*, Phys. Rev. B **22**, 904 (1980).
[27] Z. M. Li, V. N. Popov, and Z. K. Tang, Solid State Commun. **130**, 657 (2004).
[28] M. Mohr *et al.*, Phys. Rev. B **76**, 035439 (2007).
[29] R. B. Capaz *et al.*, Phys. Rev. B **74**, 121401(R) (2006).
[30] V. Perebeinos, J. Tersoff, and P. Avouris, Phys. Rev. Lett. **92**, 257402 (2004); for simplicity we use identical power-law dependencies for both the bright and $K$-momentum excitons.
[31] Tentative assignment of the (10, 0) peak follows $(2n + m)$ PL trends in a similarly prepared HiPCO sample.